Progressive Collapse Resistance to Axially-Restrained Frame Beams. Paper by Youpo Su, Ying Tian, and Xiaosheng Song

Discussion by Weijian Yi, Qingfeng He, and Xiao Yang

College of Civil Engineering, Hunan University, Changsha, Hunan, China

The paper presents the experimental results of a series of 12 reinforced concrete (RC) beams restrained longitudinally against axial deformation. Some theoretical considerations are also proposed on the basis of a theory developed by Park and Gamble.[13] The innovative design of the experiments and testing results presented by the authors allowed the discussers to investigate the compressive arch action and tensile catenary action in reinforced concrete beams. The discussers would like to offer the following comments and suggestions:

1. As seen in Fig. 2 to 4, there should be a great rigid assembly to block horizontal displacement of the specimens under compressive arch thrust. Also, the horizontal force should be measured. It is noted that from Fig. 5 to 9 that several axial force curves take on slippage in the position of zero axial force. This slippage may have resulted from an experimental device other than the behavior of the beams. In addition, the linear variable differential transformer (LVDT) installed in the actuator can only be used to measure the cylinder displacement of the actuator rather than the displacement of the beam. From Fig. 4 it can be seen that the steel frame on which the actuator was fixed may also deform upward under loading. The displacement of the actuator's cylinder is not equal to the displacement of the specimen. It is necessary to calibrate the flexibility of the frame, then subtract the displacement of the frame from the total actuator's displacement to obtain the displacement of the specimen. In addition, the sudden drop of the load-carrying capacity in Specimens A3 and A6, as shown in Fig. 5 and 8, is perhaps due to the sudden release of elastic strain energy stored in the frame in the conversion process of arch action to catenary action. If the stiffness of the test device was large enough, more smooth curves[13] could be obtained.

2. In Fig. 5 to 8 and Fig. 12, the load-deflection curves are marked with a yielding point, which means that the yielding of tension steel reinforcement occurred at the supports; however, how to measure the strain of the steel was not described in the paper. It is not clear how to get the yielding point in the testing. From the curves in these figures, such as Specimens A1, A4, B3, B4, and others, it cannot be considered that the behavior of the specimens at the yielding point have not been beyond the "linear load-deflection response," assuming the yielding bending moment amplifies the factor of Specimen B3 at the midspan and support as 1.15 and 1.65, respectively (Fig. 12). The estimated yield load according to Eq. (3) is at least 10% less than that listed in Table 3. In testing the applied load, the axial force and bending moment at the supports could be measured. Then, the bending moment at the midspan could be calculated based on Eq. (3). The yielding of steel reinforcement, however, can only be determined from the measured strain of the steel. The measured strain of the steel was not listed in the paper, possibly due to limits on length. The authors could plot the

measured strain of the steel of Specimen B3 in the Closure of this discussion, which would be helpful in better understanding the paper.

3. In the literature to date, there are very few measurement results of arch thrust in the testing of RC beams and slabs. It is very interesting that the maximum arch thrust and the maximum load-carrying capacity of the beams occurred at a different deformation state, as described in the paper. The curves shown in Fig. 12 and Eq. (3) seem to give a reasonable explanation of the relationship between the increase in the cross section bending resistance capacity and the change in load-carrying capacity of the beam. In the compressive arch action stage, the effect of axial force on the bending resistance capacity of the sections and the flexural equilibrium state of the beam changed with deflection. For the slabs with a small section height, the stage from the beginning of the arch action to the snap-through is very short. It can be loosely considered that the sectional bending resistance capacity and the load-carrying capacity of the slab reach the maximum at the same time, but the section height of a beam is usually much greater than that of a slab. Before the cross section bending resistance capacity reaches its maximum, the beam reaches the maximum load-carrying capacity. This is the main difference in compressive arch action between beams and slabs. It is also the main finding of the paper. Unfortunately, the paper gives the measured relative bending moment of only one specimen. The variation of arch thrust is limited to qualitative discussions. Using Eq. (3) in the paper, Park and Gamble[13] developed an arch thrust equation of a slab strip, as shown in Eq. (1) of the paper. Park's equation, however, implies an assumption that the "maximum load-carrying capacity and the maximum arch thrust occurred at the same time." Park's model is not applicable to the beams presented in the paper. As shown in Fig. 12, the axial force, bending moments at the midspan, and support can be expressed as the functions of deflection δ. The correct method is to solve the deflection δ from the following equation

$$\frac{d(M + M')}{d\delta} = \frac{dN}{d\delta}\delta + N$$

By substituting δ into Eq. (3) in the paper, the maximum load-carrying capacity of the beam under the action of arch thrust can be obtained.

4. The paper states that the tension of steel reinforcement at the midspan in all of the specimens was finally fractured. For example, there were three steel bars of 14 mm (0.552 in.) diameter in the bottom of Specimen B3. The total tension force was 247 kN (55.53 kip). Due to the elongation of the steel reinforcement rate of 27%, top reinforcement should also be in tension. Therefore, the axial force in the beam may

not be less than 247 kN (55.53 kip). In Fig. 5, however, the axial force in Specimen A3 is only approximately 100 kN (22.48 kip). The axial tension forces in other specimens are also smaller than the total tension force of the bottom steel bars. In the second paragraph on p. 604, it says that "The final failure of all specimens was announced by the fracture of bottom reinforcement at the interface of beam and center column stub." According to the explanation for Fig. 12 in the paper, the bending moment in the midspan existed until the bottom steel reinforcement fractured. This is possible because the bottom and top steel bars are in different tension stress states, which results in a bending-tension state. If there is a considerable bending moment at the midspan of a beam in the final stage, the load-carrying capacity of the beam is obviously underestimated by the model presented in Fig. 14 because there is not only catenary action but also bending moment in the load path. As described in the paper, "It is noted that, prior to failure, the specimen could still resist a significant amount of bending moment at the critical sections. Therefore, a double curvature deformed shape was maintained in the beams until failure when the bottom reinforcement at the midspan fractured under catenary action" (first paragraph, p. 606). This description may be used to explain why the measured axial force is less than the total tension force in the bottom steel reinforcement of the beam. If this explanation was acceptable, the ultimate load-carrying capacity would be calculated using Eq. (3) in the paper by simply substituting the measured axial tensile force and bending moments in the equation. In this way, however, the comparison shown in Fig. 14 may be meaningless. In addition, "tensile arch action" in Table 3 should be "tensile catenary action."

5. A comparison of the test curves of Specimens B2 and B3 is very interesting because Specimen B2 contains only one more bottom steel bar of 14 mm (0.552 in.) diameter than Specimen B3. According to the curves illustrated in Fig. 7 and 8, the curves of Specimens B2 and B3 are drawn together, as shown in Fig. 15. It is indicated in the figure that Specimens B2 and B3 have an approximate yield load and ultimate load (a difference of approximately 10%), and the same maximum arch thrust of 210 kN (47.21 kip). The significant difference is the conversion from compressive arch action to tensile catenary action. When the relative deflection reached 0.7, the compressive arch action disappeared in Specimen B2. At this time, the top steel reinforcement at midspan had not yet reached the position below the bottom steel reinforcement at the support. The "arch" should be maintained at this stage. In Specimen B3, however, the compressive arch action existed until the relative deflection reached beyond 1.10. At this stage, the top face at the midspan of the beam had dropped below the bottom face at the support. In the two specimens, the transition from "arch" to "catenary" could not be explained by existing models.

AUTHORS' CLOSURE

The authors would like to thank the discussers for their interest in the paper. The paper focused primarily on the effects of compressive arch action on the load-carrying capacity of axially restrained frame beams.

It appears that the discussers have misunderstood the context regarding the measurement of beam deflections. The paper states that "the vertical load P and deflection δ at the center column stub were measured by a built-in load cell within the actuator and displacement transducers." The
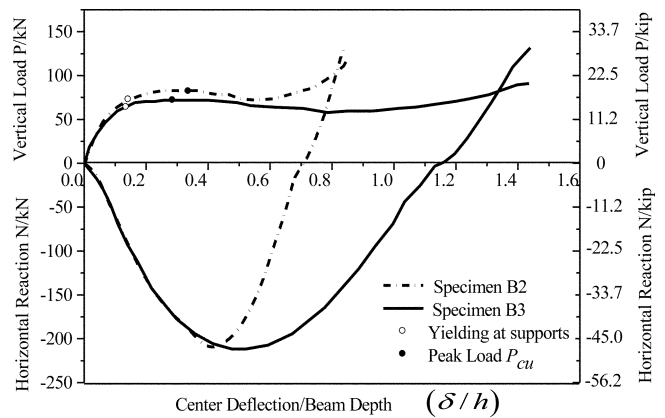

Fig. 15—Vertical load and horizontal reaction force versus normalized center deflection (Specimens B3 and B2).

vertical load P was measured solely by the load cell of the actuator. However, as indicated by the use of "transducers" in this sentence, the center vertical displacement was measured by more than one transducer. Two LVDTs were actually used in the tests: one was mounted at the actuator and another one was independent. The difference in the measurements from these two transducers was negligible at the peak load for each specimen, indicating that the loading frame placed vertically was sufficiently stiff.

A sudden drop of loads occurred mainly in testing Specimens A2, A3, A5, and A6 with small span-depth ratios. Such a phenomenon can be better explained by the notable effects of high axial forces developed in the beams on their flexural strength rather than the strain energy stored in the vertical loading frame. A numerical model with properly defined parameters can successfully capture the sudden loss of loading capacity as a result of concrete crushing. The horizontal rigidity of the supports that anchored the beams was in a realistic range that the neighboring structural components such as columns and slabs can offer to a frame beam. A test setup with extremely high axial rigidity is neither practical in a test nor necessary for simulating the actual boundary condition of a frame beam. Slippage in the measured horizontal reaction force took place when the compressive arch action was transformed into catenary action. Such a phenomenon can be explained by the inherent tolerance for the connection components of the supports, especially at the pins connecting the steel sockets with the test bed. The slippage was sufficiently small, thereby causing negligible effects on the overall performance of the specimens.

Table 3 provides the measured horizontal reaction force and vertical deflection of specimens at the reach of peak load P_{cu} under compressive arch action. The discussers may have misinterpreted P_{cu} as the load causing tensile steel yielding. Because P_{cu} was much higher than the yield load, it is not surprising that the "estimated yield load according to Eq. (3) is at least 10% less than that listed in Table 3."

The discussers claim, without providing experimental evidence, that "For the slabs with small section height, the stage from the beginning of arch action to snap-through is very short. It can be loosely considered that the sectional bending-resistance capacity and the load-carrying capacity of the slab reach the maximum at the same time." The major difference between the beam and one-way slab is the span-depth ratio that is one of the parameters governing the effects of compressive arch action. It is noteworthy, however, that

the same mechanism of compressive arch action can still be assumed for both beams and one-way slabs. Additionally, due to the secondary effects resulting from large slab deformation far beyond initial steel yielding, the slab loading capacity can be reached earlier than its flexural capacity. Such a performance has also been observed in the beam tests (such as Specimen B3). The authors extended the model developed for one-way slabs by Park and Gamble[13] to axially restrained beams. It is noted that, different from what the discussers have interpreted, Eq. (1) defines P as the vertical load applied on the beam rather than as the "arch thrust." In addition, scrutinizing the context of Chapter 12 of Reference 13 indicates that no assumption was adopted or implied by the authors of this reference about a simultaneous reach of the maximum vertical load-carrying capacity and the maximum axial force developed in the beams under compressive membrane action.

The discussers briefly described an approach to calculate the beam loading capacity P_{cu}. This approach is simply a different mathematical method to solve the same problem: searching the maximum load at varying values. The equation provided by the discussers can be derived from Eq. (3) by taking the first-order directive of P with respect to δ as zero. Despite the seemingly simple format of this equation, no detailed formulations are provided by the discussers to define M, M', and N as a function of δ. It is possible that a closed-form solution of δ cannot be obtained and a numerical

approach has to be used to determine the value of δ at P_{cu}. Additionally, if the same ways of defining M, M', and N (as those recommended by Park and Gamble[13]) are used, it is believed that the approach recommended by the discussers would lead to results identical to the analytical predictions given in the paper.

It is noted that N is defined in the paper as the measured horizontal reaction force. Hence, Fig. 5 to 8 show the horizontal reaction force rather than the axial force actually developed in the beams. At large deformation of beams subjected to catenary action, the axial force will be much higher than the horizontal reaction force. Therefore, it is inappropriate to directly correlate the forces shown in these figures to the catenary action forces. Figure 14 shows a simple model for predicting the loading capacity as well as the comparison between the calculated and measured results. As described in the paper and admitted by the discussers, the internal force may be far more complicated than that assumed in the simple model. By presenting Fig. 14, the authors used a modest way to show their disagreement with this simple model, which has been adopted in Reference 10, and alert readers that this model may result in unreliable predictions.

The authors agree that the test results for Specimens B2 and B3 are interesting, especially the earlier transition from a compressive arch action to a catenary action in Specimen B2. The authors are currently carrying out an analytical study that may facilitate a reasonable explanation of the different

---

Carbon Fiber-Reinforced Polymer for Continuity in Existing Reinforced Concrete Buildings Vulnerable to Collapse. Paper by Sarah Orton, James O. Jirsa, and Oguzhan Bayrak

Discussion by Rafael Alves de Souza

ACI member, PhD, Universidade Estadual de Maringá, Maringá, Brazil

The authors have made a significant contribution regarding the strengthening of structures to prevent progressive collapse. Also, the authors have presented an interesting strategy based on the use of carbon fiber-reinforced polymers (CFRPs). Despite the quality of their research and their valuable findings, the discusser requests clarification on some topics.

INTRODUCTION AND RESEARCH SIGNIFICANCE

The authors have proposed the use of FRP as a strengthening alternative for beams that might lose some of their supports (interior columns). It is undoubtedly a situation that may occur in daily practice and engineers need to come up with quick and rational strategies of strengthening. The engineering solutions are desired to be simple, fast, and economical to avoid progressive collapse and allow the users to escape or recover their belongings before the effects become significant.

The use of CFRP for critical situations such as that presented by the authors, however, does not seem to be a practical alternative, as this solution may demand specialized workers (adequate intervention) and structural engineers (design of the CFRP sheets). From a practical point of view—despite the exceptional qualities of CFRP sheets—a shoring approach using steel or wood shores will work better for a provisory situation where the loss of some columns is evident. Also, this kind of approach is cheaper, faster, and does not require a complex background. Could the authors explain

the main advantages of using CFRP instead of shoring elements in critical situations where progressive collapse is evident?

EXPERIMENTAL PROCEDURE

The authors have determined a strengthening scheme using FRP that would allow a beam with discontinuity reinforcement to survive loss of a column. For that, they have investigated seven half-scale specimens based on typical information obtained from constructions built in the 1970s. Unfortunately, the concrete compressive strength used for the specimens do not represent the majority of the buildings constructed in that time. Also, the values presented in Table 3 are very different and may prompt distortions regarding the interpretation of the results.

The discusser does not agree with the procedure of taking just one specimen for each proposed situation (NR-2, PM-1, PM-2, NM-1, NM-2, FR-1, CR-1). At least two specimens should have been tested for each situation to effectively discuss the results based on a minimum statistical background. Also, there is a great variation for the compressive concrete strength used in all specimens. As one can see in Table 3, Specimens NM-2, FR-1, and CR-1 have concrete compressive strengths that are significantly higher than the other situations. Additionally, some specimens are significantly more reinforced than others and, taking into account the great variation regarding the concrete compressive strength and reinforcements (steel and FRP), some results were expected.

EXPERIMENTAL RESULTS AND DISCUSSION

To the discusser's understanding, the authors have mentioned two basic situations of failure for their specimens: flexure strength and catenary (or cable) action. However, it is not clear throughout the paper which situation is more effective for representing the level of strength of a structure based on the GSA guidelines.[1] Also, it is not clear when catenary (or cable) action may develop. How can the rotation of 0.13 radians be defined to obtain catenary (or cable) action?

In the situation denominated "flexural strengthening," the authors used 4.5 times the amount of CFRP used in Specimen NM-2. Why not use the same strengthening used in Specimens PM-1/PM-2 and NM-1/NM-2 to account for the effect of providing FRP for positive and negative moments? Increasing CFRP in Specimen FR-1 makes a comparison with Specimens PM-1, PM-2, NM-1 and NM-2 difficult. Also, in Table 3, there is no description regarding the concrete compressive strength of Specimen NM-1.

CONCLUSIONS

The authors have presented a very interesting paper concerning the progressive collapse of reinforced concrete structures. The loss of a supporting column may leave a beam unable to resist gravity loads and may lead to the collapse of either side of the lost column. In that way, engineers need to come up with techniques that allow building occupants to recover their belongings or escape before the effects of a local failure become significant. The authors have presented a technique based on the use of CFRP sheets, which can be considered a very effective intervention because it can provide a great level of ductility for damaged sections.

In critical situations, however, this alternative of intervention may be considered more complicated and expensive than other provisory and simple situations, such as a shoring approach (steel or wood). Also, when strengthening a beam for flexure using CFRP, one must be aware of the effective shear strength. If the shear strength needs to be enhanced once the flexural strength was increased by using CFRP sheets, this solution may become even more expensive and complicated, demanding special attention.

The authors are correct when they state that a statically applied load corresponding to 2(DL + 0.25LL), based on GSA guidelines,[1] may or may not correspond to actual progressive collapse prevention. In fact, new information concerning catenary (or cable) action is needed to better understand the maximum strength of reinforced concrete structures.

Finally, the discussed paper presents the importance of providing continuity for positive and negative reinforcements. It is an issue that requires special attention in the design codes. Practical experience has been shown through the years that an adequately detailed structure may withstand incredible loads, even if some errors were committed during the design process. There is no doubt that the proposed intervention using FRP sheets is effective; however, it will only be possible in practice if an adequate continuity of reinforcement was defined in the damaged structure.

AUTHORS' CLOSURE

The authors thank the discusser for his interest in the paper. It appears the discusser misinterpreted the intent of the strengthening procedure. The objective was to prevent a progressive collapse if a catastrophic event occurred. The technique was never intended to be used on a structure that was heavily damaged and needed to be shored to prevent collapse.

The application of CFRP in these situations does require specialized fiber workers and structural engineers, but there is not a lack of these qualified people. The use of CFRP to strengthen structures has been long implemented and there are several firms that provide both the engineering assistance to design the CFRP and the workers to correctly apply it. CFRP is both flexible and lightweight so that after the surface preparation, the application of the fabric can occur in less than a few hours with only a few skilled workers. For the beams in this study, the CFRP application only took approximately 1 hour.

For this study, the intent was to see whether CFRP could be applied in such a way to provide continuity (which it can) and whether that continuity can aid in the resistance of progressive collapse (which it can). Although it would have been desirable to repeat the tests of some CFRP designs, that was simply not within the time or budget constraints of the projects. The evaluation of more variables was deemed more important than replicating rather expensive test specimens. Specimens NM-1 and NM-2 did replicate results of the negative moment strengthening. The two specimens were the same, with the only difference being in the amount of CFRP applied. After the successful test of Specimen NM-1, it was decided that a reduced amount of CFRP could produce the same results, so Specimen NM-2 was tested.

The design concrete strength for the specimens was 27.6 MPa (4000 psi). The concrete, provided by a local concrete supplier, was unusually low for the first batch of beams, and high for the second two. The concrete compressive strength of Specimen NM-1 was 33.8 MPa (4900 psi) (the same as for Specimens PM-1 and PM-2). Although the concrete strength may not have been as intended, it did not significantly affect the behavior of the specimens. For a specimen under catenary action, the most important variables are the location and strength of the reinforcing steel, and height and depth of the beam. As for the steel in the specimens, all specimens have the same reinforcing steel and the same steel design, except Specimen CR-1, which was designed using current ACI 318 requirements for integrity reinforcement.

All specimens (except for Specimen FR-1) exhibited some form of flexural failure (ex-beam hinging at the support in Specimens NM-1 and NM-2), then went into catenary action. Catenary action consistently developed at a deflection equal to, or just greater than, the depth of the beam. To reach this deflection without a complete flexural failure (bar fracture), the beams needed to have sufficient rotational ductility. For these specimens, the rotational ductility needed to be approximately 0.13 radians.

For Specimen FR-1, the intent was to increase the flexural strength of the beam to allow it to carry the moments induced by a loss column. This was not the same intent as the other specimens, so a different design approach was used. The design of the CFRP was based on basic flexural principles and used the least amount of CFRP needed to reach the required strength. As seen in Fig. 12 of Reference 19, the strains measured in the CFRP were approaching the fracture strain and most of the CFRP had debonded, indicating that the CFRP was almost fully used.

The discusser is correct that shear strength must be considered. Improving the continuity in a beam does not help if the shear strength is lacking. Strengthening for shear was outside of the scope of the research project.

REFERENCES
19. Orton, S. L.; Jirsa, J. O.; and Bayrak, O., "Design Considerations of Carbon Fiber Anchors," *Journal for Composites for Construction*, ASCE, V. 12, No. 6, Nov/Dec 2008, pp. 608-616.

New Formula to Calculate Minimum Flexure Reinforcement for Thick High-Strength Concrete Plates. Paper by E. Rizk and H. Marzouk

Discussion by Abdulkadir Cevik

Assistant Professor, Department of Civil Engineering, University of Gaziantep, Gaziantep, Turkey

The authors have proposed a new equation to calculate minimum flexure reinforcement for thick plates and two-way slabs. The validity of the new proposed equation is verified by a comparison between the proposed equation with Battista's experimental results and with different code formulas for calculating minimum reinforcement for flexural members. At first sight, everything seems to be correct; however, after closer inspection, the database (Battista's experimental results) used for verification cannot be used for this purpose. First of all, the range of the dependent variable (steel ratio) is too close where steel ratios are 0.22, 0.23, and 0.24, respectively. On the other hand, the ranges of independent variables are quite high as compared to the dependent variable, which means that most of the dependent variables do not have any significant effect on the dependent variable. As the dependent variable is grouped and the interaction diagrams are plotted, this problem can be observed easily, as shown in Fig. 10 to 12. As can be seen, variations of related independent variables have no effect on the dependent variable (steel ratio).

As a result of the aforementioned arguments, Battista's experimental results cannot be used to verify any code formulations or equations regarding the calculation of minimum flexure reinforcement for thick plates and two-way slabs.

AUTHORS' CLOSURE
The authors would like to thank the discusser for his interest in the paper, and for providing the authors the opportunity to illustrate a few details. The developed model is based on the theoretical assumptions based on the theory of plates in Eq. (12) to (17) and the shear sandwich model simplification, not any test data as explained in the paper. The test data of Battista is not related to the paper.

The discusser is arguing that Battista's experimental work cannot be used to verify any code formulations or equations regarding the calculation of minimum flexure reinforcement for thick plates and two-way slabs, because most of the independent variables (concrete compressive strength f_c', steel yield strength f_y, and slab depth d) do not have any significant effect on the dependant variable (reinforcement ratio ρ).

The discusser's argument is not correct because he ignored the size-scale effect factor as an independent factor on the amount of reinforcement ratio. It is possible to consider the structural member size effect on the minimum reinforcement ratio through the brittleness number concept N_P, as defined by Bosco et al.[15] The brittleness number is derived from linear elastic fracture mechanics (LEFM) concepts, as

$$N_P = \rho \frac{f_y h^{0.5}}{K_{IC}} \tag{39}$$

where ρ is the steel reinforcement ratio, K_{IC} is the concrete fracture toughness, f_y is the yield strength of the steel, and h is the thickness of the structural member.
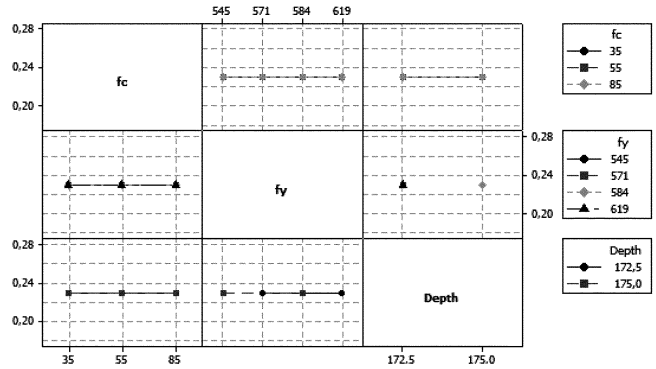

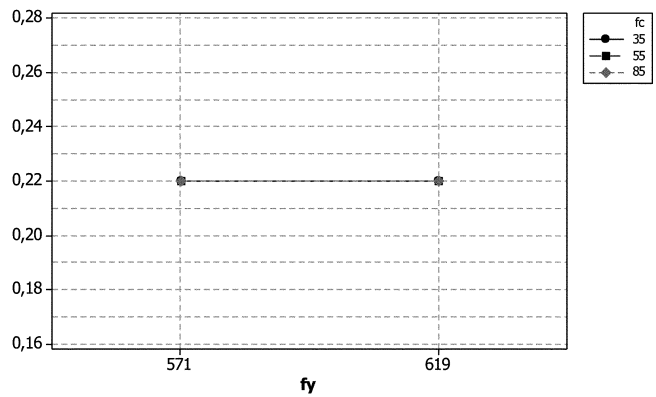Fig. 10—Interaction plot of steel ratio = 0.23 for f_c versus f_y, f_c versus depth, and depth versus f_y.

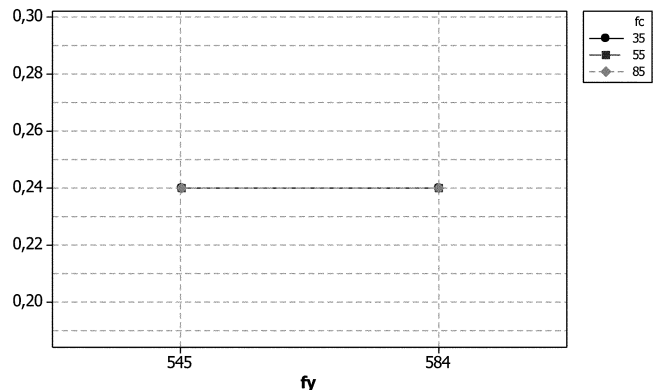Fig. 11—Interaction plot of steel ratio = 0.22 for f_c versus f_y.

Fig. 12—Interaction plot of steel ratio = 0.24 for f_c versus f_y.

The critical value of the stress-intensity factor K_{IC} can be evaluated as follows
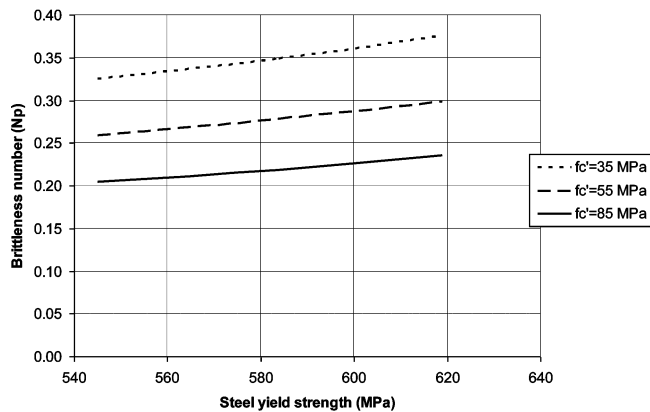
$$K_{IC} = \sqrt{G_f E_c} \tag{40}$$

Fig. 13—Brittleness number (N_P): steel yield strength for steel reinforcement ratio = 0.23%. (Note: 1 MPa = 145 psi.)
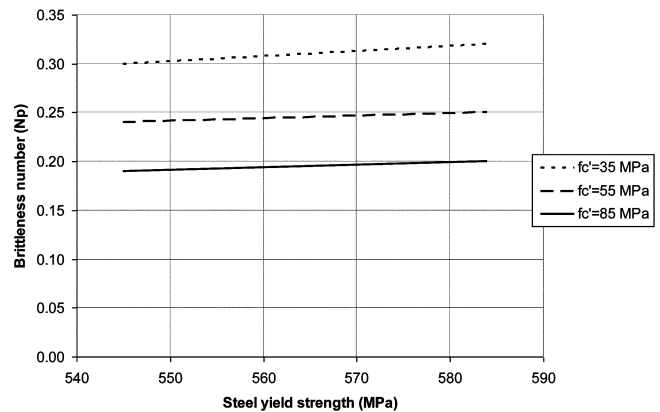

Fig. 15—Brittleness number (N_P): steel yield strength for steel reinforcement ratio = 0.24%. (Note: 1 MPa = 145 psi.)
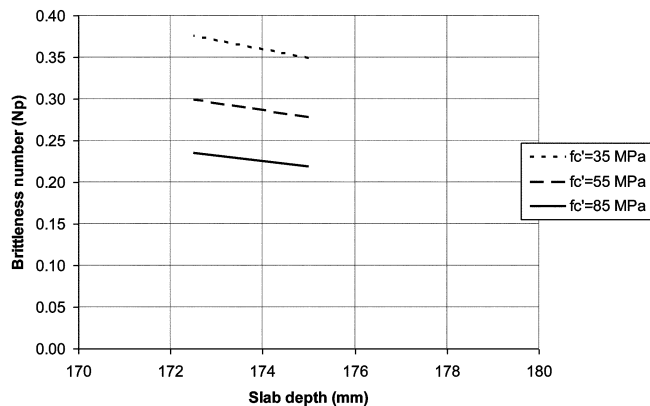

Fig. 14—Brittleness number (N_P): slab depth for steel reinforcement ratio = 0.23%. (Note: 1 MPa = 145 psi.)
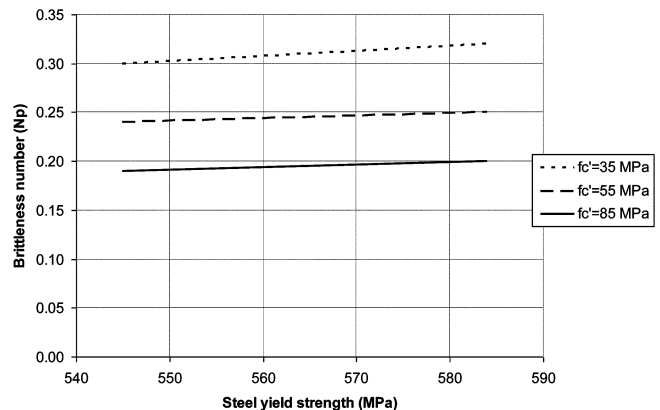

Fig. 16—Brittleness number (N_P): steel yield strength for steel reinforcement ratio = 0.22%. (Note: 1 MPa = 145 psi.)

where G_f is the fracture energy and E_c is the concrete modulus of elasticity determined by standard methods. The brittleness of the structural member increases by increasing the member size or decreasing the steel reinforcement ratio. Bosco et al.[15] found that a particular value of number N_P does exist, for which the moment at which the reinforcement yields equals the moment at first cracking. Such a condition defines the minimum amount of reinforcement ratio. Current design codes suggest a constant minimum reinforcement ratio independent of member size. This is not true as the minimum reinforcement ratio is inversely proportional to the member depth.

As a result of the aforementioned arguments, Battista's experimental results can be used to verify any code formulations or equations regarding the calculation of minimum flexure reinforcement for thick plates and two-way slabs. The significance of the independent variables on the reinforcement ratio is clear and can be observed easily, as shown in Fig. 13 to 16.

Evaluation of Load Transfer and Strut Strength of Deep Beams with Short Longitudinal Bar Anchorages.
Paper by Sergio F. Breña and Nathan C. Roy

Discussion by Dipak Kumar Sahoo, Bhupinder Singh, and Pradeep Bhargava

PhD, Reader, School of Engineering, Cochin University of Science and Technology, Kochi, Kerala, India; PhD, ACI member, Assistant Professor, Department of Civil Engineering, Indian Institute of Technology Roorkee, Roorkee, India; PhD, Professor, Department of Civil Engineering, Indian Institute of Technology Roorkee

The authors are to be complimented for the interesting study. Based on *a/d* ratio, the authors have sought to identify two mechanisms of load transfer in deep beams: tied-arch mechanism and truss mechanism. It is well established, however, that besides the ratio, the truss mechanism is also dependent on the amount of web reinforcement in the deep beam, whereas the tied-arch mechanism is relatively independent of the amount of web reinforcement. The presence of web reinforcement, however, does serve to confine the inclined strut in the tied arch. Further, ACI 318-08 specifies that diagonal struts in beams inclined in the range of 25 to 65 degrees with the adjoining tie are well-conditioned for strut-and-tie modeling. Therefore, for all cases wherein the inclination of the strut is typically more than 25 degrees (that is, *a/d* < 2.14), it will be reasonable to use the tied-arch mechanism as the overarching method for the analysis of deep beams.

The authors have rightly observed that although vertical web reinforcement is explicitly included in truss models, it is not done so in tied-arch models. Moreover, the effect of horizontal web reinforcement is usually not included in either of the models. The discussers feel that discounting the role of horizontal web reinforcement runs contrary to a unified approach to strut-and-tie modeling. On the basis of their investigations of statically determinate truss models with vertical and with horizontal truss mechanisms, Matamoros and Wong (2003) have concluded that though both the mechanisms yield conservative results, they require almost double the amount of web reinforcement compared to an indeterminate truss model consisting of a combination of the vertical and horizontal truss models. The discussers are of the opinion that for *a/d* less than about 2.14 (strut inclination >25 degrees), it will be simple and convenient to adopt the tied-arch mechanism with web reinforcement—both vertical and horizontal—being accounted for in determining the strength of the single bottle-shaped diagonal strut joining the load point and the support.

The term *F* in Eq. (12) and (18) should be corrected to $F_{S\text{-}truss}$. The discussers suggest that the issue of apportioning the total shear between the tied-arch and the truss mechanism can probably be better resolved by using the combined indeterminate strut-and-tie model of Fig. 7(a) rather than the determinate model approach implied in Eq. (10) through (21). Furthermore, the authors' attempt to determine the fraction of the shear transferred through truss action on the basis of strain measurements using Instruments L2 and L3 may not be reliable because the strain profile across the strut axis is nonuniform due to the bottling effect.

It is interesting to note that the strut efficiency factor β_s of the diagonal struts of the nine beams that failed by strut failure when plotted against the corresponding strut inclination angle α is seen to be increasing with increasing α following the linear trend shown in Fig. 12. On the other hand, irrespective of the angle of inclination of the diagonal strut with the adjoining horizontal tie, ACI 318-08 Appendix A recommends a constant strut efficiency factor of 0.75 for all of these reinforced bottle-shaped struts. For strut inclinations smaller than approximately 30 degrees, Fig. 12 shows that the ACI recommended strut efficiency factor may be unconservative when compared to the experimental results of the authors. Interestingly, for all of these beams, including those with short anchorage lengths, the authors' experimentally observed strut efficiency factors do have a sufficient margin of safety when compared with the predicted strut efficiency factors obtained from a recent model by Sahoo (2009), shown as follows.

$$\beta_s = \left(0.60 + \frac{0.05}{r_c} + 55\rho_T\right)\frac{\alpha}{90} \qquad (22)$$

In Eq. (22), (valid for up to 81 MPa [11,748.05 psi]), α is the angle of inclination of the diagonal strut with the tie in degrees, and r_c is the concentration ratio of the load resisted by the diagonal strut obtained as the ratio of $w_{s\text{-}top}$ and half the strut length. The effective transverse reinforcement ratio ρ_T is computed from the corrected version of the transformation used in ACI Eq. (A-4), shown as follows (Sahoo et al. 2009)
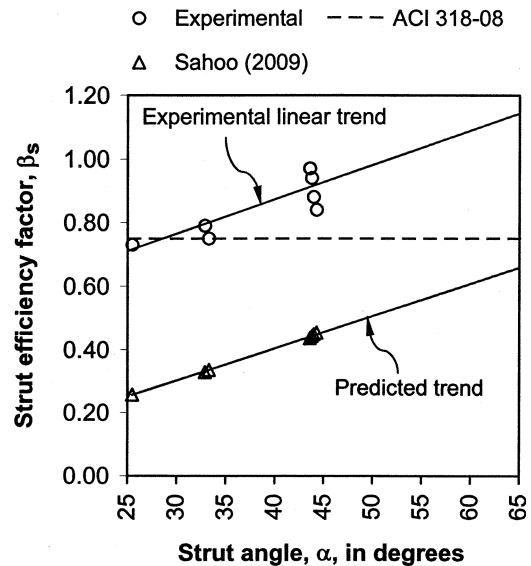

Fig. 12—Variation of strut efficiency factor with strut angle.

$$\rho_T = \sum \frac{A_{si}}{b_s s_i}\sin^2\alpha_i \qquad (23)$$

where A_{si} is the cross-sectional area of each layer of web reinforcement in the *i*-th orientation; b_s is the strut or beam thickness (out-of-plane); s_i is the spacing of web reinforcement in the *i*-th orientation; and α_i is the angle between the strut and the bars in the *i*-th orientation.

What is notable in Fig. 12 is that that the trend of the authors' experimentally obtained strut efficiency factors is similar to the trend of the predicted strut efficiency factors based on the Sahoo (2009) model.

REFERENCES
Matamoros, A. B., and Wong, K. H., 2003, "Design of Simply Supported Deep Beams Using Strut-and-Tie Models," *ACI Structural Journal*, V. 100, No. 6, Nov.-Dec., pp. 704-712.

Sahoo, D. K., 2009, "An Investigation of the Strength of Bottle-Shaped Struts," PhD thesis, Indian Institute of Technology Roorkee, Roorkee, India, 324 pp.

Sahoo, D. K.; Singh, B.; and Bhargava, P., 2009, "An Appraisal of the ACI Strut Efficiency Factors," *Magazine of Concrete Research*, V. 61, No. 6, Aug., pp. 445-456.

AUTHORS' CLOSURE
The authors appreciate the discussers' interest in their paper. We would first like to thank the discussers for pointing out notation errors in Eq. (12) and (18) in the paper. This allows us to correct these equations and fix other errors found in the manuscript. Figure 11(b) should be modified to be consistent with the notation given in Fig. 11(a) included in this discussion.

$$F_{C(L)} = F_{C(R)} - F_{S\text{-}truss}\cos\gamma \qquad (12)$$

$$V_{truss} = F_{S\text{-}truss}\sin\gamma \qquad (18)$$

Finally, the values reported in the last column of Table 3 are ratios of calculated-to-test values of stresses in the strut for a tied-arch model. Therefore, the header for the last column in Table 3 should be modified to read $f_{S\text{-}TA}/f_{S\text{-}TA(test)}$.

The authors would now like to provide closing comments in response to points made by the discussers. The discussers correctly point out that the load-transfer mechanism in deep beams is not only influenced by a/d, but also by the amount of transverse web reinforcement. To isolate the influence of a/d in the load-transfer mechanism, the authors designed the deep beams in our tests with the same amount and spacing of transverse reinforcement. The main objective of the research was to identify the effect of short bar anchorage at the support on the load-transfer mechanism. Certainly a more complete study would include variations in the amount and spacing of transverse reinforcement while holding a/d constant—this was, however, outside the scope of our tests.

The discussers point out that by using the minimum permissible angle between a strut and a tie in accordance with ACI 318-08, one could determine a maximum a/d of 2.14, where load could be transferred directly into the support using a tied-arch model. Although one could certainly design a beam that falls in this a/d range using only a tied-arch model and in compliance with ACI 318-08, loads can also be transferred indirectly into the support through truss action for a/d less than 2.0, as has been previously demonstrated (refer to Eq. (4) from FIP [1999] in the paper). Furthermore, the authors contend that in the case of deep beams with anchorage details that do not ensure yielding of the bottom tie at the face of the extended nodal zone above the support (a requirement needed to satisfy equilibrium in a tied-arch model), the fraction of load transferred through truss action might be higher than for a beam with appropriate anchorage in this region, provided that enough transverse reinforcement exists to support this load transferred by truss action. The fact that specimens having longitudinal bar anchorages shorter than required to develop yielding of the bottom tie were able to support loads comparable with those with full development demonstrates that a fraction of the total load was being transferred through a truss mechanism.

The discussers point out that it would be better to use an indeterminate strut-and-tie model involving tied-arch and truss mechanisms to determine the fraction of shear transferred by each model. The authors would like to remind the discussers that, to solve an indeterminate strut-and-tie model, one must either assume the fraction of load transferred by each individual mechanism or determine this load fraction in proportion to the individual submodel stiffnesses. The best way to verify our experimental results was to separate the problem into two statically determinate models where the load being transferred could be verified by independent measurements taken during the tests. These results were intended to provide information on the fraction of load being transferred by each potential load-transfer mechanism to provide guidance for the future use of indeterminate models for this type of structure. The load carried by each mechanism was estimated through independent experimental measurements taken along the direction of struts in the assumed tied-arch and truss models for each group of beams. The authors would like to emphasize that we were using potentiometers that measured the overall axial shortening of the relevant struts (the potentiometer ends were attached to points located at the ends of struts). This allowed us to experimentally determine the average axial force-displacement relationship of each strut and avoid basing our results on local strain readings. The total load (sum of forces carried by each individual mechanism) would of course have to add to 100% of the applied shear. If the total load carried did not add to
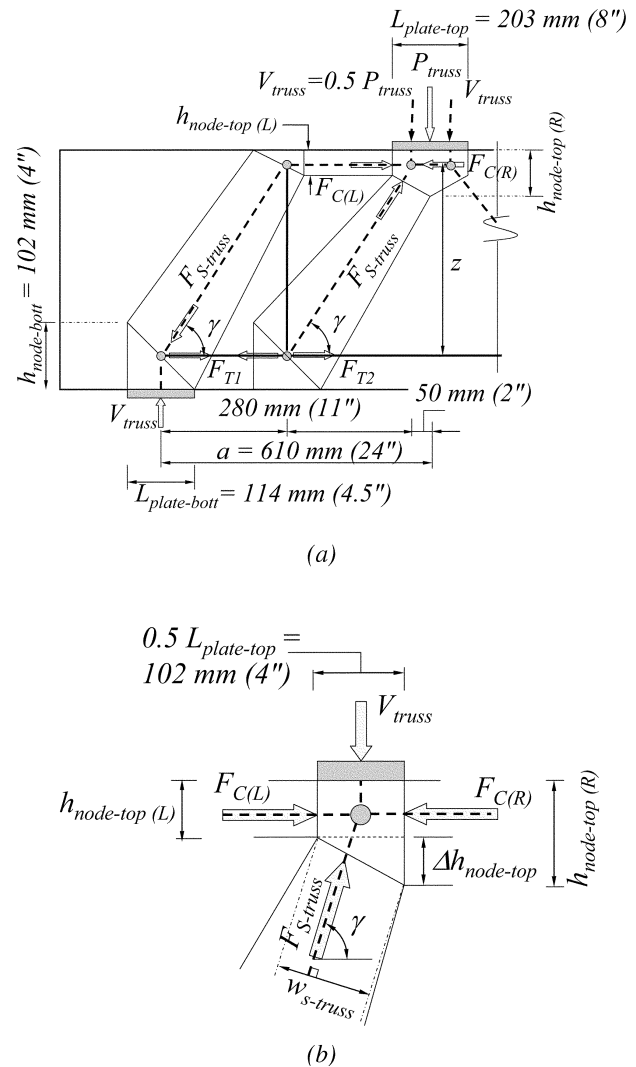

(a)

(b)

Fig. 11—(revised from original paper)—Truss model for load transfer: (a) geometry of model; and (b) top node details.

100% of the applied shear, that would mean that the adopted procedure to determine the individual load-transfer fractions was flawed or that experimental measurements were not reliable. As mentioned in the paper and included in Table 3, the largest difference between the load needed to be transferred by tied-arch action to ensure that 100% of the applied shear was carried and the load determined through potentiometer measurements was approximately 12%. We believe that this small difference gives reasonable confidence about the procedure employed to estimate the fraction of load transferred by tied-arch and truss mechanisms.

The variation of strut efficiency factor β_s that the discussers present in Fig. 12 is consistent with results plotted in Fig. 9. The main difference is that β_s is plotted in Fig. 9 as a function of a/d instead of direct strut angle α, but these two quantities are directly related. The authors are also quite satisfied that the experimentally determined β_s values follow the same trend as the discussers' model. We thank the discussers for making us aware of their model and look forward to studying the reference they provided in detail.

Punching Strength of Reinforced Concrete Footings. Paper by Josef Hegger, Marcus Ricker, and Alaa G. Sherif

Discussion by Andor Windisch
ACI member, PhD, Karlsfeld, Germany

The authors should be complimented for their interesting test series and informative report. The saw cuts of different test specimens (Fig. 5) especially allow for very informative insights into the failure process of the footings and some shortages of the code provisions.

The footings without shear reinforcement did not fail in direct punching: the failure was caused by the failure of the anchorage of the flexural reinforcement along the perimeter of the specimens. This can be observed at the horizontal cracking along/above the flexural reinforcement at the edges of the specimens and at the many failing outer corners of practically each and every footing without shear reinforcement. These local failures could partly be caused by the loading pattern with the sliding bearings near edges modeling a uniform surface load, which is practical for test reasons but not realistic. These circumstances could lead to a decision not to consider these specimens in the discussion. Nevertheless, as the detailing of the reinforcement corresponds to the practice, it is mandatory to tackle the results as they help to elucidate the shortages of the code provisions.

EXPERIMENTAL PROGRAM
Material properties
It is not clear at which age the test specimens were loaded. Was it around the 28th day?

Test setup
Even if Fig. 4(b) does not yield detailed information about the real loading pattern, the discusser has the impression that the specimens of Series II were relatively overloaded along their perimeter; the outer sliding bearings were too near to the edges of the specimens.

The locations of the flexural steel strain gauges as shown in Fig. 4(b) are not optimal. At choosing these locations, the staggering of the tension line due to the shear force (refer to the inclined cracks in Fig. 5), too, should have been taken into consideration.

EXPERIMENTAL RESULTS
Cracking and failure characteristics
All test specimens without shear reinforcement failed due to the failure of the anchorage of the flexural reinforcement. The authors declare correctly that "the failure occurred along/due to the wide shear crack and the inclination of the cracks in these specimens is determined by the ratio a/d." The saw cuts of the uniformly loaded footings with shear reinforcement reveal an extremely important and forward-looking fact: as the inner work required to open the outer shear crack crossing the shear reinforcement was higher than the inner work causing the much steeper inner shear crack, even though the shear reinforcement was activated, it determined the position of the failure surface but not the size of the ultimate failure load. The authors correctly specify that "in contrast to the footings without shear reinforcement, the influence of a/d on the inclination of the shear cracks

seems to be negligible." The distance s_0, the spacing between the column face and the first row of shear reinforcement is decisive.

Steel strains
As revealed before, the position of the strain gauges was not optimal. The flexural steel strains measured at failure of the footings with shear reinforcement reached yielding as the shear reinforcement let the inner crack develop in the neighborhood of the strain gauges.

DISCUSSION OF EXPERIMENTAL RESULTS
Effect of a/d
The slenderness ratio a/d is an indirect indicator of the possible inclination of the failure shear surface only. At this point, a direct factor (the inclination) should be introduced in the codes.

Effect of concrete compressive strength
The authors' conclusion is correct: the behavior of the footings can not be described by a strut-and-tie model. The failure load in shear is not controlled at all by the bearing capacity of the compressive strut. The "source" of the ultimate load in shear is the shear load-bearing capacity of the concrete compressive zone. Before the failure occurs, the shear crack, as part of the failure surface, is so wide that no aggregate interlock or similar sidelines could be drawn on to explain the behavior. The influence of the increasing concrete strength is neither linear nor follows any square root relationship. Further fundamental research is needed regarding this.

Effect of shear reinforcement
As explained previously, at least in case of Specimens DF16 to DF18, the shear reinforcement was not activated as part of the shear load-bearing mechanism; hence, any conclusion—for example, based on Fig. 10—would be misleading.

Effect of soil-structure interaction
It is a pity that the saw cut of the test specimen with shear reinforcement, Specimen DF 9, supported on sand, was not presented in the paper.

COMPARISON OF PREDICTIONS AND EXPERIMENTAL RESULTS
Comparison with ACI 318-08
Figure 12(b) seems to confirm that ACI 318-08 does not consider the influence of a/d. Nevertheless, the real influence of the effective depth, as shown in Fig. 12(a), should not be evaluated without considering the impact of a/d, that is, the inclination of the failure surface. The specimens supported on sand with different effective depths had different a/d too. The position of the critical perimeter b_0, accompanied with the assumption of the uniform soil pressure distribution,
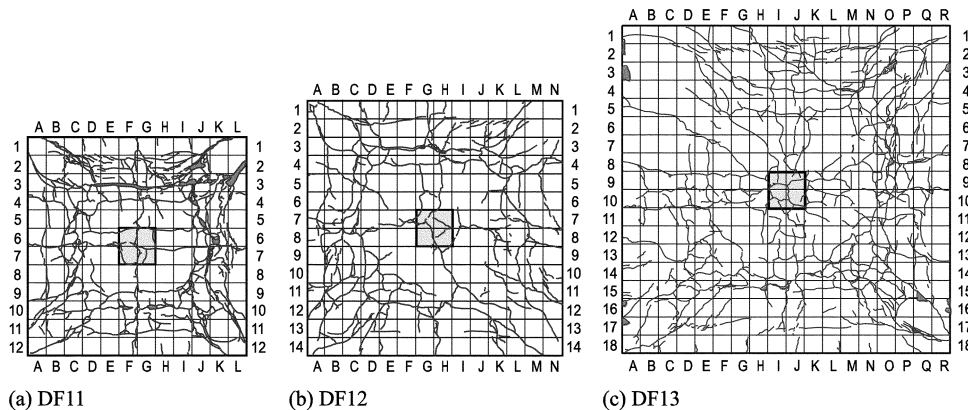
(a) DF11   (b) DF12   (c) DF13

Fig. 16—Crack patterns of Footings DF11 to DF13 after failure.

approximates the real behavior on the safe side (namely, conservative) two times; refer to the crack pattern in Fig. 5(iv) (Fig. 5(h) shows Specimens DF7, not DF17). The crack pattern of Specimen DF9 should have been shown, too, to realize the impact of the shear reinforcement on the failure behavior of sand-supported footings.

Comparison with Eurocode 2
The authors are correct in that:
- The failure crack patterns of the footings without shear reinforcement seem to prove the position of the basis control perimeter at 2.0d distance from the column face; and
- It is odd that $V_{Ru,max}$ according to Eq. (17) controls the design. Being only a function of the concrete compressive strength, it seems to refer to a web-crushing limit although, in case of the tested footings, no crushing could occur.

The authors criticize that $V_{Ru,max}$ does not reflect a/d correctly. The discusser agrees and suggests that in the case of footings, a control like $V_{Ru,max}$ has no meaning at all. Instead of $V_{Rd,max}$, the authors propose a new equation, Eq. (19), which is a follow-up of Eq. (15). It would be informative to learn how the multiplier $16\sqrt{(d/u_0)}$ has been found. Whereas $v_{Rd,c}$ (Eq. (15)) yields a lower limit, $V_{Rd,max}$ (Eq. (19)) sets an upper limit of the load-bearing capacity. Comparing Eq. (19) to Eq. (15), the margin between them seems to originate from the geometry, that is, $\sqrt{(d/u_0)}$. Why does the geometry not influence the punching shear-stress resistance $v_{Rd,c}$ either? The authors are kindly asked to clarify. It would be desirable, too, that the odd "best fit" form of $(100\rho \cdot f_{ck})^{1/3}$ in Eq. (15) will be substituted with a physically sound term in the New Model Code of *fib* under preparation.

Even if—according to Fig. 15(d)—Eq. (19) seems to yield a "safe" upper limit, the rate of approximation depends on a/d and is, in the case of footings supported on sand, very conservative. For the time being, the limited number of the test specimens with shear reinforcement, that is, with different ratios d/u_0 and different spacings between the column face and the first row of shear reinforcement, s_0, do not allow for final acceptance of the proposed $V_{Rd,max}$ (Eq. (19)).

The authors are kindly encouraged to continue their interesting research work.

AUTHORS' CLOSURE
The authors are grateful for the comments and the interest in the paper. In the present closure, the authors would like to

address some of the points raised in the discussion to provide some clarification. Because of space limitations, the most important points, such as the type of failure, will be discussed in more detail.

EXPERIMENTAL PROGRAM
Failure characteristics
The discusser assumes that the failure of the footings without shear reinforcement was caused by bond failure. This is not correct. In Fig. 16, the crack patterns of three footings without shear reinforcement are presented. All footings were loaded via 16 bearings, simulating a uniform load case. The crack patterns are typical for a punching shear failure. At first, radial cracks around the column appeared, then the first tangential cracks developed at the column face and, later on, at higher load stages, more and more tangential cracks appeared. The ultimate punching capacity of the slab was achieved when the inclined failure crack reached the flexural reinforcement. Because the failure was relatively brittle and the tests were load controlled, it was not always possible to stop the test right in time. After the failure took place, the load was removed and, afterward, the specimens were reloaded to determine the bearing capacity after punching failure. During this second loading phase, the flexural reinforcement was heavily deformed in the region of the failure crack, which led to the spalling concrete at some edges.

In contrast to Fig. 2, in the footings without shear reinforcement, the flexural reinforcement was twice bent-up (Fig. 17). Thus, for the given geometry, a typical bond failure is nearly impossible. The footings with shear reinforcement were identical to the specimens without shear reinforcement in terms of flexural reinforcement and concrete strength. Although the anchorage of the flexural reinforcement was weaker (90-degree hooks), the specimens with shear reinforcement reached a higher failure load. This should clearly indicate that at least the footings without shear reinforcement and 180 (2 times 90) degree hooks did not fail prematurely by bond failure. Hallgren et al.[5] reported the results of 14 punching shear tests on reinforced column footings. In these tests, among other parameters, the influence of the end anchorage of reinforcement was investigated systematically. Hallgren et al.[5] concluded that the anchorage of the flexural reinforcement has only a small influence on the punching strength of footings; however, curved anchorage improved the ductility. It is worth mentioning that the Swedish saw cuts and crack patterns are very similar to those
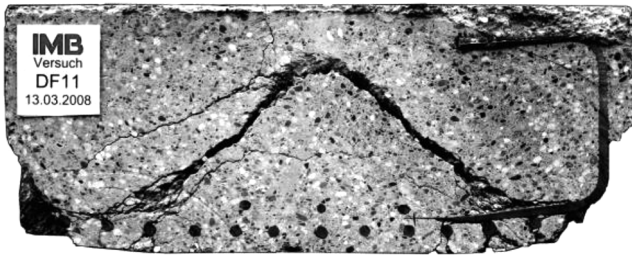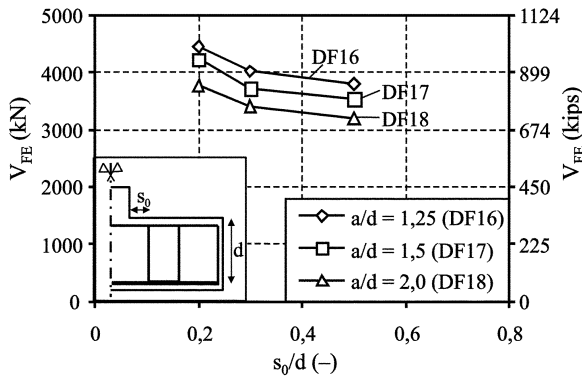
Fig. 17—Saw cut of Footing DF11.

Fig. 18—Result of finite element calculations performed to investigate influence of distance from column face to first row of shear reinforcement s_0 on failure load.
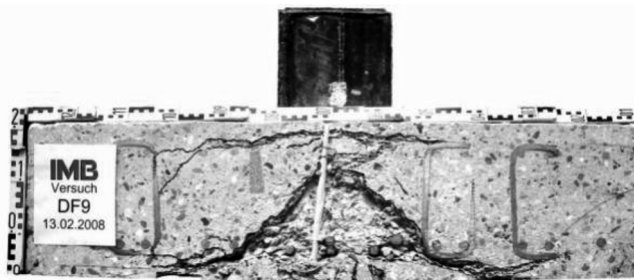

Fig. 19—Saw cut of Footing DF9.

in the present tests and also showed spalling concrete at the edges of the specimens.

For the footings with shear reinforcement, the discusser correctly mentions that the shear reinforcement determined the position of the failure surface but not the value of the ultimate failure load. The discusser also correctly presumed

that the failure load is sensitive to the spacing between the column face and the first row of shear reinforcement s_0. To investigate this effect in more detail, Ricker[14] conducted a finite element analysis. In Fig. 18, the calculated failure loads V_{FE} are plotted against s_0/d (with d being the effective depth). The finite element analysis showed that a reduction of the spacing between the column face and the first row to $s_0 = 0.2d$ leads to an increase in failure load between 10 and 14%. However, to clarify the influence of this parameter, further tests are needed.

Figure 19 presents the saw cut of Specimen DF9 with shear reinforcement (supported on sand). The crack pattern is comparable to those of the uniformly loaded specimens. The concrete is slightly more crushed because the specimen was overloaded when the bearing capacity after failure was determined during a second loading phase. The inclination of the failure shear crack is very steep (approximately 50 to 60 degrees). The crack propagates from the column face to the anchorage of the first row of shear reinforcement consisting of stirrups.

COMPARISON OF PREDICTIONS AND EXPERIMENTAL RESULTS

The equation for the calculation of the maximum punching capacity was originally derived for flat plates by a regression analysis.[15] For the present paper, this equation was adapted to footings. Due to a lack of suitable tests, Eq. (19) was adapted in such a way to determine lower-bound values for the maximum punching-shear capacity of footings as correctly mentioned by the discusser. According to Eurocode 2, a critical perimeter at the periphery of the loaded area was chosen for the calculation of the maximum punching-shear capacity. In contrast, the punching-shear resistance without shear reinforcement, according to Eq. (15), is verified at control perimeters within $2.0d$. The use of a relatively large distance to the control perimeter has the advantage that the correlation with test data over the normal range of column dimensions to effective depth is reasonable (refer to Reference 11). This can be explained by a reduction of the influence of the uneven shear stress distribution resulting from the type of column (for example, circular or rectangular) and the column dimensions. Thus, for control perimeters far away from the periphery of the loaded area, the column dimensions need not be considered directly.

REFERENCES
14. Ricker, M., "Zur Zuverlässigkeit der Bemessung gegen Durchstanzen bei Einzelfundamenten," doctoral thesis, RWTH Aachen University, Aachen, Germany, 2009, 304 pp.

15. Hegger, J.; Häusler, F.; and Ricker, M., "Zur Durchstanzbemessung von Flachdecken nach Eurocode 2," *Beton- und Stahlbetonbau*, V. 103, No. 2, Feb. 2008, pp. 93-102.